www.elsevier.com/locate/jmbbm

Composite scaffolds for controlled drug release: Role of the polyurethane nanoparticles on the physical properties and cell behaviour

Piergiorgio Gentile, Devis Bellucci, Antonella Sola, Clara Mattu, Valeria Cannillo, Gianluca Ciardelli

PII: S1751-6161(14)00396-8
DOI: http://dx.doi.org/10.1016/j.jmbbm.2014.12.017
Reference: JMBBM1349

To appear in: *Journal of the Mechanical Behavior of Biomedical Materials*

Received date: 8 September 2014
Revised date: 15 December 2014
Accepted date:
16 December 2014

Cite this article as: Piergiorgio Gentile, Devis Bellucci, Antonella Sola, Clara Mattu, Valeria Cannillo, Gianluca Ciardelli, Composite scaffolds for controlled drug release: Role of the polyurethane nanoparticles on the physical properties and cell behaviour, *Journal of the Mechanical Behavior of Biomedical Materials,* http://dx.doi.org/10.1016/j.jmbbm.2014.12.017

Composite scaffolds for controlled drug release: role of the polyurethane nanoparticles on the physical properties and cell behaviour

Piergiorgio Gentile[1,2]*, Devis Bellucci[3], Antonella Sola[3], Clara Mattu[2], Valeria Cannillo[3], Gianluca Ciardelli[2]

[1] School of Clinical Dentistry, University of Sheffield, 19 Claremont Crescent, Sheffield S102TA, United Kingdom;

[2] Politecnico di Torino, Department of Mechanical and Aerospace Engineering, Corso Duca degli Abruzzi 24, Turin 10129, Italy;

[3] University of Modena and Reggio Emilia, Department of Engineering "E. Ferrari", Via Pietro Vivarelli 10, Modena 41125, Italy;

* Author to whom correspondence should be addressed; e-mail: p.gentile@sheffield.ac.uk.

Tel.: +44-(0)114-2717938; Fax: +44-(0)114-2265484.

Abstract

Localised delivery of appropriate biomolecule/drug(s) can be suitable to prevent postoperative infections and inflammation after scaffold implantation *in vivo*. In this study composite shell scaffolds, based on an internally produced bioactive glass and a commercial hydroxyapatite, were surface coated with an uniform polymeric layer, embedded with thermo-stable polyesterurethane (PU)-based nanoparticles (NPs), containing an anti-inflammatory drug (*indomethacin*; IDCM). The obtained functionalised scaffolds were subjected to physico-mechanical and biological characterisations. The results indicated that NPs incorporation into the gelatin coating of the composite scaffolds: 1) not changed significantly the micro-architecture of the scaffolds in terms of mean pore diameter and pore size distribution; 2) increased the compressive modulus; and 3) allowed to a sustained IDMC release (65-70% of the loaded-drug) within the first week of incubation in physiological solution. On the other hand, the NPs incorporation did not affect the biocompatibility of composite scaffolds, as evidenced by viability and alkaline phosphatase (ALP) activity of MG63 human osteoblast-like cells.

Keywords: Bone tissue engineering; composite scaffolds; gelatin coating; indomethacin; nanoparticles.

1. Introduction

Tissue engineering aims to restore and maintain the function of damaged or diseased human bone tissues by combining biodegradable scaffolds with isolated functional cells and signalling molecules, such as growth factors (Langer and Vacanti, 1993). An ideal scaffold to be employed in bone tissue regeneration and repair should be biocompatible, highly porous with a morphology resembling the microstructure of trabecular bone, osteoconductive and biodegradable, and should have adequate mechanical strength, sufficient to ensure mechanical stability prior to synthesis of new extracellular matrix by seeded cells (Rezwan et al., 2006). Both calcium phosphates, in particular hydroxyapatite (HA), and bioactive glasses have been extensively used in the last years as scaffolding materials, tissue surgery and dentistry. HA is chemically and structurally similar to the mineral component of human bone and it is able to create a bond with the surrounding bone tissue *in vivo* (Orlovskii et al., 2002). On the other hand, HA degradation rate after implantation in the body is remarkably low, and this is an undesirable feature for the realisation of scaffolds, which are expected to be resorbed *in vivo* at rates appropriate to new tissue regeneration (Ducheyne et al., 1993; Oonishi et al., 2000). Moreover, the production of HA based scaffolds requires high temperature thermal treatments, which may lead to HA decomposition with the formation of CaO, α- or β- tricalcium phosphate, and their presence produces decohesion of the whole material, hinders sintering and modifies the biodegradability of the final product (Cihlar et al., 1999; Suchanek et al., 1997). Bioactive glasses offer important advantages as an alternative to HA, mainly due to their higher bioactivity index. Specific compositions, such as the so-called 45S5 Bioglass®, are able to bond to hard tissues as well as to soft ones, to stimulate angiogenesis and osteoblast turnover (Day, 2005; Xynos et al., 2000). A fundamental research topic is the design and development of new composite systems, which combine a bioglass and a calcium-phosphate phase, in order to overcome the intrinsic limits of the single constituents. In this sense, several works have been devoted to investigate the sintering and mechanical behaviour of HA with phosphate or silicate-based bioglass addictions (Bellucci et al., 2011b; Bellucci et al., 2013b; Goller et al., 2003;

Ravarian et al., 2010). Recently a novel binary composite ("HA_BGCaM") has been obtained by sintering a CaO-rich bioglass (named BG_Ca/Mix), characterised by a low tendency to crystallise, with the addition of HA as the second phase (Bellucci et al., 2013a). Thanks to the peculiarities of the glass (Bellucci et al., 2010; Bellucci et al., 2012b), it was possible to treat the composites at a relatively low temperature (818 ^{o}C), thus minimising the interaction between the constituent phases and avoiding HA decomposition. Moreover, the obtained composite has been successfully employed to realise scaffolds for bone tissue engineering by means of a protocol recently developed to go beyond the limits of the conventional replica technique. The new samples, called "shell scaffolds", were characterised by an internal high porosity combined with an external resistant and permeable surface, which ensures an adequate mechanical strength (Bellucci et al., 2012a).

As a further step, composites based on bioceramics and natural polymers can be developed in order to reproduce at best the natural bone structure, which is composed by a mineral phase (biological HA) and collagen. These new generation scaffolds are able to preserve the structural and biological functions of bone tissue in a biomimetic way. Among them, gelatin is a non-expensive and commercially available biomaterial that has gained interest in biomedical engineering, mainly because of its biodegradability. Gelatin is obtained by thermal denaturation or physical and chemical degradation of collagen, the most widespread protein in the body, occurring in most connective tissues as skin, tendon and bone. With respect to collagen, gelatin does not express antigenicity in physiological conditions, it is completely resorbable *in vivo* and its physicochemical properties can be suitably modulated. The main limitation of gelatin for the production of tissue substitutes arises from its rapid dissolution in aqueous environments (Huang et al., 2005). Chemical and physical crosslinking methods have been used to increase gelatin stability in aqueous media (Ciardelli et al., 2010; Kuijpers et al., 2000); Genipin, the aglycone of geniposide (an iridoid glucoside isolated from the fruits of *Genipa Americana* and *Gardenia jasminoides Ellis*) is a naturally occurring compound that can be used as a coupling agent for amino containing materials (Tonda-Turo et al., 2011). Genipin has been widely used as a crosslinking agent for natural

polymers in tissue engineering and biomedicine. For example, genipin was used to crosslink (1) gelatin microcapsules for drug delivery (Chen et al., 2010; Huang et al., 2009), (2) gelatin conduits for peripheral nerve regeneration (Chen et al., 2005) and (3) composite films based on gelatin and hydroxyapatite/bioactive glass for bone tissue engineering (Gentile et al., 2010).

Recently a feasibility study has been devoted to discuss 45S5 Bioglass®-derived shell scaffolds coated by bio-resorbable gelatin (Bellucci et al., 2012c). Unfortunately, the uncoated scaffolds were completely crystallized, since high temperatures are required in order to consolidate 45S5 (Boccaccini et al., 2007; Chen et al., 2006a). On the other hand, the main objective was to investigate the effect of the biomimetic coating either on scaffolds' porosity and on their bioactivity *in vitro*. In this sense, *in vitro* tests in a Simulated Body Fluid solution confirmed the bioactivity of the gelatin-coated samples, whose porosity remained open and interconnected.

Here, for the first time, HA_BGCaM binary composite powders have been employed to produce gelatin-coated shell scaffolds, according to the protocol developed in (Bellucci et al., 2012c). In order to investigate potential applications of a gelatin coating as drug-delivery, thermo-stable polyesterurethane (PU)-based nanoparticles containing an anti-inflammatory drug, indomethacin (IDMC), were incorporated during the fabrication of the polymeric coating to fix the location of nanoparticles within the porous composite scaffolds, with the aim to prevent postoperative infections and inflammation after scaffold implantation *in vivo*.

IDMC is a non-steroidal anti-inflammatory drug with a high relevance in the treatment of disorders like several kind of arthritis, pericarditis, bursitis, tendinitis or spondylitis. Approved by FDA in 1965, it is widely used due to its antipyretic and analgesic properties, more potent than aspirin (Manjoo et al., 2010; Temussi et al., 2011). Its chemical structure is presented in Figure 1.

Furthermore, the effect of PU nanoparticles incorporation on the physical and biological properties of the coated composite scaffold(s) were investigated by analysing the scaffold micro-architecture, porosity, chemical composition, cell attachment, cell viability and ALP activity using MG63 human

osteoblast-like cells. Then, the drug release was analysed to evaluate the therapeutic potential of the functionalised coated scaffold(s).

2. Materials and Methods

2.1 Production of composite scaffolds

HA_BGCaM composite powders were prepared according to the protocol described in (Bellucci et al., 2013a). Briefly, laboratory produced BG_Ca/Mix glass powders (Bellucci et al., 2011a; Bellucci et al., 2012b), sieved to a grain size below 45 μm, were mixed with proper amounts of commercial HA powders (CAPTAL® Hydroxylapatite, Plasma Biotal Ltd, UK), in order to prepare a composite with the following composition: 70 wt.% BG_Ca/Mix and 30 wt.% HA powders. Then, HA_BGCaM powders were used to produce bioceramic shell scaffolds. The steps to realise these samples are just summarised here, since they have been reported in detail elsewhere (Bellucci et al., 2012a). 51 wt.% distilled water, 34 wt.% HA_BGCaM powders, 5 wt.% polyethylene powder and 10 wt.% polyvinylic binder were mixed in a beaker for 1 h in order to prepare a ceramic slurry. Polyurethane sponges were then rapidly immersed in the slurry, extracted without squeezing and dried in a multidirectional air flux at 100 °C. Subsequently the impregnated sponges were heat-treated in a muffle kiln at 818 °C for 3 h (the following thermal cycle was employed: from room temperature to 500 °C at 5 °C/min; from 500 °C to the final temperature at 10 °C/min) with the aim to sinter the composite structure and to decompose the organic phase (i.e. the polyethylene powders and the polymer skeleton). Finally, the scaffolds were extracted from the furnace and let to cool down naturally.

2.2 Production of PU nanoparticles

Nanoparticles (NPs) were prepared according the protocol described in (Mattu et al., 2013). Briefly, NPs were prepared with a novel polyesterurethane NS-HC2000, in the following referred as PU_1. The acronym represents the components of the material: NS is the chain extender (n-BOC-serinol), H corresponds to the diisocyanate (HDI) and C2000 indicates the macrodiol (PCL-diol with a

molecular weight of 2000 g/mol). The polymer was synthesised according to a two-step polymerisation reaction, as reported by Mattu et al. (Mattu et al., 2012). IDMC-loaded NPs (5 wt.%) were prepared by the single emulsion solvent evaporation method, by selecting Ethyl Acetate (Sigma-Aldrich, Italy) as solvent and PVA (Poly-Vinyl alcohol; Sigma-Aldrich, Italy) as emulsifier. The PU (100 mg) and the IDMC (5 wt.%, Sigma-Aldrich, Italy) were dissolved in ethyl acetate (4 ml) and added dropwise into water (4 ml) containing the emulsifier, under sonication. The primary emulsion was then poured into 50 ml of water containing PVA, to favour polymer precipitation and solvent evaporation. Particles were then collected and washed by centrifugation (10000 rpm for 20 min).

Particles size, surface charge and polydispersity index (PDI) were characterized by Dynamic light scattering (Malvern Instruments) and IDMC encapsulation efficiency (EE) was determined by UV spectroscopy (Perkin Elmer Lambda 25) at 320 nm. Briefly, 10 mg of lyophilized drug-loaded NPs were fully dissolved in ethyl acetate. The solvent was then completely evaporated and the drug extracted with a solution of ethanol and water (3:1) for UV analysis. EE was calculated using the following formula:

$$EE = Dm/Dt \times 100$$

where Dm is the amount of drug contained in 10 mg of NPs, measured by UV, and Dt is the theoretical amount of drug that is expected in 10 mg of NPs (5 wt.%).

2.3 Surface coating of gelatin embedded with PU nanoparticles on composites scaffolds

The sintered porous scaffolds were deaerated and infiltrated with a 5% wt/v gelatin solution (G; Type A, Sigma-Aldrich, Italy), incorporating 5 wt.% drug loaded nanoparticles. Then, the composite scaffolds were immersed for 15 minutes under continuous stirring into the gelatin solution, and dried in an air-circulating oven at room temperature. The dipping procedure was repeated for 5 times and, then each coated scaffold was immersed into 10 ml of 5% wt/w genipin (GP) solution (Challenge Bioproducts, Taiwan) for 24 h at 37 °C to obtain stable coating by

crosslinking gelatin. According to previous studies (Tonda-Turo et al., 2011), genipin was chosen to confirm the gelatin crosslinking, thanks to the blue colouring obtained by spontaneous reaction of genipin with amino acids and proteins, containing amino groups.

2.4 Characterisation of the functionalised coating on composite scaffolds

2.4.1 Microstructural characterisation

The surface morphology of the obtained scaffolds was observed with a scanning electron microscope, SEM (Philips XL-20 and FEG-SEM Nova NanoSEM 450-FEI for lower and higher magnification, respectively) after gold coating (Emscope SC 500A Sputter Coater). SEM was operated at accelerating voltage of 15 kV, while FEG-SEM at 1.0 kV.

2.4.2 Fourier transform infrared-attenuated total reflectance spectroscopy (FTIR-ATR)

Chemical analysis of functionalised coated scaffolds was performed by ATR-FTIR spectroscopy over a range of 4000–550 cm^{-1} using a Perkin Elmer equipment (resolution 4 cm^{-1}; 32 scans).

2.4.3 Mechanical tests

The mechanical properties of the scaffolds were measured under compression test using a mechanical testing machine (Instron 858; Eden Prairie, MN, USA). Three samples (15mm x 17mm x 15mm size) were evaluated for each type (before and after coating). The samples were tested at room temperature. The cross-head speed was set at 0.01 $mm \cdot s^{-1}$.

2.4.4 In vitro drug release tests

Functionalised composite scaffolds of (1.5 × 1.5 × 1 cm) were immersed in glass vials containing 10 mL PBS. The vials were sealed to minimise the changes in the initial pH and incubated at 37°C without stirring. The blank control (pure composite scaffolds) was done under the same experimental conditions with the absence of IDMC. Two milliliters of the release medium was withdrawn periodically and replaced with an equivalent volume of fresh buffer. Three replicates

were measured, and the results were averaged with standard deviation. The amount of drug released was determined with an ultraviolet (UV) spectrophotometer at 320 nm.

2.4.5 Cell tests

MG-63 osteoblast-like cells (ATCC, Rockville, MD) were grown in a controlled atmosphere (5% CO_2; T= 37 °C) in Dulbecco's modified eagle's medium (DMEM, Sigma-Aldrich, UK) supplemented with 10% fetal bovine serum (FBS), 1% nonessential amino acids (Gibco, Italy), 2.0 mM L-glutamine (Gibco), and 1% antibiotics (penicillin–streptomycin, Gibco). After thawing, cells were routinely split 1:10 every 3–4 days and used between the 3rd and 4th passages.

Before cell seeding, material samples (1.5 × 1.5 × 1 cm) were sterilized in a 70% ethyl alcohol solution (EtOH, Sigma-Aldrich, UK) for 30 min, washed in PBS and incubated with an appropriate medium for 3 h. The medium was then discarded. MG-63 cells were detached using 0.25% trypsin in 1 mM ethylenediaminetetraacetic acid (Sigma-Aldrich, UK) and seeded on composite sponges and in 24-well polystyrene tissue culture plates (TCPs) as controls at a density of 7.5 x 10^3 cells/cm^2.

After incubation (1, 4 and 7 days), the medium was removed; 200 µL of 3-dimethylthiazol-2,5-diphenyltetrazolium bromide (MTT; Sigma-Aldrich, UK) solution (5 mg/mL in DMEM without phenol red) and 1.8 mL of DMEM were added to the cell monolayers; the multiwell plates were incubated at 37 °C for further 4 h. After discarding the supernatants, the dark blue formazan crystals were dissolved by adding 2 mL of solvent (4% HCl 1N in isopropanol, Sigma-Aldrich, UK) and quantified spectrophotometrically (Tecan Infinite M200) at 570 and 690 nm. In the control cultures, the cells were placed directly into 24-well polystyrene culture plates at the same culture density as placed onto the samples. The mean and the standard deviations were obtained from three different experiments on the same specimen.

Alkaline phosphatase (ALP) activity (after 14 days of cell seeding) was measured by incubating 100 µL of each samples with 0.5 mL alkaline buffer solution (Sigma-Aldrich, UK) and 0.5 mL of stock

substrate solution (40 mg p-nitrophenyl phosphate disodium, Sigma-Aldrich, UK), diluted in 10 mL of distilled water, at 37 °C for 1 h. Production of p-nitrophenol in the presence of ALP was measured by monitoring light absorbance of the solution at 410 nm using a spectrophotometer. The mean and the standard deviation were obtained from three different experiments. Results were reported as International Units (IU/L).

2.5 Statistical analysis

Experiments were run at least in triplicate for each sample. All data were expressed as mean ± SD. Statistical analysis was determined by using Analyse-it v2.22 software. The statistical differences between groups were calculated using Kruskal-Wallis One Way Analysis of Variance on Ranks (ANOVA). Statistical significance was declared at $p<0.05$.

3. Results and discussion

On the basis of the excellent preliminary results obtained by (1) the morphological and mechanical characterisation of shell scaffolds (Bellucci et al., 2012a) and (2) the preliminary gelatin coated hybrid samples (Bellucci et al., 2012c), the aim of this work was not only to mimic the complex bone morphology and its structure, but also to introduce an appropriate anti-inflammatory drug (IDMC) to reduce the risk of implant failures associated to infections or inflammatory processes, that are related to the *in vivo* implantation of the scaffolds. Polyesterurethane IDMC-loaded NPs were introduced into the gelatin coating, since nanocarriers improve the control over the release kinetics of the encapsulated drugs, whilst protecting it from degradation and prolonging its activity *in vivo*. Mean size of plain and IDMC loaded-NPs was 196 ± 2 nm and 195 ± 3 nm, respectively, while PDI was 0.12 ± 0.01 and 0.1 ± 0.01. IDMC encapsulation efficiency was 89 ± 2.3%. IDMC encapsulation did not lead to any significant variation in NPs size or polydispersity index, indicating that the anti-inflammatory drug did not affect the size distribution of the carriers as found in literature (Kim et al., 2000).

Figure 2 shows some micrographs of the shell composite scaffold internal structure after coating with gelatin embedded with IDCM-loaded PU nanoparticles. An uniform polymeric layer coated the internal surface of pores and their struts. In particular, the natural polymer adhered to the walls of pores without reducing the total porosity, with open and fully interconnected pores (Figure 2(A)). Moreover, the presence of the NPs in the polymeric coating was verified by FEG-SEM microscopy (Figure 2(B)), that demonstrated that NPs were distributed on the surface without altering the porous structure or closing the pores. It is possible that the negatively charged NPs surface (-10 ± 0.2 mV) led to their adsorption on the gelatin-modified composite scaffolds.

FTIR-ATR analysis was performed to confirm the obtainment of the functionalised coating on the scaffold walls. Figure 3 show the chemical structure of the composite (A) and functionalised (B) scaffolds. The FTIR spectrum of the composite scaffold revealed the typical band of silica-based bioactive glasses and hydroxyapatite (Kazarian et al., 2004; Krajewski et al., 2005): wide vibrational bands corresponding to Si-O-Si stretch and Si-O-Si bending at 1060 cm^{-1} were overlapped with the characteristic bands of hydroxyapatite, corresponding to the P-O bending vibrations $\nu_3(PO)_4$ (broad band 1040–1090 cm^{-1}); while the vibrational band at 900–950 cm^{-1} has been credited to the presence of silanol groups (Si-OH) and the vibrational peak at 962 cm^{-1}, and the peaks at 602 and 571 cm^{-1} were related to the P-O bending vibrations, $\nu_1(PO)_4$ and $\nu_4(PO)_4$, respectively. On the other hand, in Figure 3(B), the characteristic gelatin bands of amide A, amide I and II, at 3350-3400, 1650 and 1550 cm^{-1} are evidenced (Tonda-Turo et al., 2011). Then, the observation of the characteristic bands of PU at 3333 cm^{-1} (urethane group), and 1293 and 1164 cm^{-1} (C–O and C–C stretching in the PCL crystalline and amorphous phase, respectively) confirmed the PU-based NPs into the functionalised surface of the scaffolds. However, no other PU characteristic bands are evidenced due to the overlap with the G coating and composite scaffold bands.

Figure 4 shows the typical compression stress–strain curve of the scaffolds before and after gelatin coating embedded with IDMC-loaded NPs. As described in previous studies (Bellucci et al., 2010;

Vitale-Brovarone et al., 2008), the compressive stress–strain curves are characterised by three distinct regions: a linear region with a moderate stress increase in the 0–15-20 % strain range (region I), a zone where stress rapidly increases due to the higher ability of the scaffold to bear loads (region II) and a third region (over 30% strain), in which the densification of the fractured scaffold (region III) occured. As described in a previous work (Bellucci et al., 2012a), the scaffolds mainly tend to crack in the outer shell of the microstructure, causing the apparent stress to drop temporarily (compressive stress in the range of 0.3–0.4 MPa in region I). However, the scaffolds maintained their ability to bear high loads, as shown by the significant increase of stress (compressive stress in the range of 0.4–0.5 MPa in region II) due to the internal porous sponge-like structure of the composite scaffolds. Moreover, compression tests on the functionalised composite scaffolds were performed in order to evaluate the effect of the gelatin coating and the incorporation of drug loaded NPs. As shown in Figure 4, the scaffolds were able to bear slightly higher loads due to the coating on the surface of the foams, causing the improvement of the mechanical properties. The compressive stress was in the range of 0.45–0.55 MPa and 0.6–0.7 MPa in region I and II, respectively. The obtained mechanical values are particularly satisfactory and confirm the positive effect of the functionalised coating on the mechanical strength of the scaffolds and it should be observed that the mechanical strength of the functionalised composite scaffolds was in the range reported for spongy bone, i.e. 0.2–4 MPa (Gibson et al., 1995).

Figure 5 shows the *in vitro* drug release, evaluated after immersion of the functionalised scaffolds in PBS for different times, showing an initial linear pattern, with about 15-20% of the drug released during the initial 3 h of incubation (burst effect), followed by a sustained IDMC release (65-70% of the loaded-drug) within the first week of incubation, with no additional release observed in the following days. In literature, different works described the release of IDMC, dispersed directly within scaffold polymer matrix, rather than encapsulated into nanocarriers (Cabezas et al., 2012; Thakur et al., 2012). As reported by Thakur et al. (Thakur et al., 2012) crosslinked gelatin sponges released no more than the 30% of the loaded drug, indicating that a substantial loss of the active

principle occurred during processing. The release was rapid and completed within the first 7 h of incubation, followed by no additional release. Recently, Ferreira et al. (Ferreira et al., 2014) showed a sustained drug release based on embedding IDMC-loaded NPs on porous PLLA scaffolds, in which 60% of the loaded-drug was released between 48 and 72 h, followed by no additional release. As obtained in this work, the presence of a polymeric coating caused a slower drug release (up to 7 days), in which the gelatin swollen network was able to entrap further the delivered IDMC from NPs.

The adhesion and proliferation of MG63 osteoblast-like cells on composite scaffolds before and after gelatin coating without/with incorporation of IDMC-loaded NPs was evaluated, with particular attention to the effect of NPs on the cell response, as for each clinical case, this parameter should be tailored to the requirements of the implantation site. The success of bone substitutive materials largely depends upon the formation of a mechanically stable and strong interface between the scaffold materials and bone tissue (LeGeros, 2002). Following the initial adhesion of cells on bone substitutive materials, a series of processes take place, affecting osteointegration and osteoconduction (Ciardelli et al., 2010). The characterisation of MG63 osteoblast-like cells behaviour was based on specific assays: MTT test to evaluate cell viability (Chen et al., 2006b), showing the cell attachment at 1 day and proliferation at 4 and 7 days; the activity of ALP was measured at 14 days to determine the bone forming potential of the cells, since ALP is regarded to be an important phenotype of bone-forming cells (Golub et al., 1992). Results of MTT and ALP activity tests on all prepared scaffolds are shown in Figure 6 and 7, respectively. The MTT test showed an increase of cell viability along the cell incubation period. In particular, cell adhesion shows no significant differences among samples at 24 h incubation. The presence of gelatin coating on the composite scaffold surface enhanced significantly the cell viability compared to their un-functionalized counterparts, as observed after 4 and 7 days of incubation. Moreover, the presence of IND-loaded PU NPs resulted in slight lower cell viability compared to functionalised scaffolds with only gelatin (MTT absorbance for coated composite scaffolds with and without NPs incorporation

were 0.43 ± 0.04 and 0.52 ± 0.03 after 7 days of cells seeding), but not interfering with the processes of migration, colonisation, adhesion and proliferation within the functionalised membranes.

ALP tests was performed to assess the bone forming potential of the cells, showing that composite scaffolds containing IND-loaded PU NPs did not affect the ALP activity of the osteoblasts (ALP value for coated composite scaffolds with and without NPs incorporation were 39.53 ± 4.89 IU/L and 44.65 ± 3.28 IU/L, respectively). In addition, the scaffold mineral content increased its stiffness which in turn modulated cell interaction with the substrate, that represents an important feature for osteoblast differentiation (Idowu et al., 2014).

4. Conclusions

Composite shell scaffolds, based on a bioactive glass (internally produced) and a commercial hydroxyapatite were successfully coated by bio-resorbable gelatin, incorporating drug loaded-PU nanoparticles: (1) to mimic the natural bone structure, which is composed by natural apatite (i.e., a mineral phase) and collagen, and (2) to obtain a controlled *in vitro* release of indomethacin. The NPs incorporation into the polymeric coating did not alter the porous scaffold structure that was characterised by open and fully interconnected pores. Furthermore, *in vitro* drug release tests revealed a 65-70% IDMC release within the first week of incubation that is suitable to prevent postoperative infections and inflammation during the next days after scaffold implantation *in vivo*. Our work also demonstrated that osteoblast-like cells on the functionalised composite scaffolds showed appropriate results in terms of viability and ALP activity of osteoblasts, and the introduction of IDMC loaded NPs did not affect the biological results. Finally, our work indicates that this biomimetic coated composite scaffolds represent a promising candidates for bone tissue regeneration, showing (1) proper porosity, pore size and mechanical properties, (2) biomimicry of bone tissue, and (3) therapeutic potential.

Acknowledgements

The authors would like to thank the FP7-PEOPLE-2011-IEF-302315-NBC-ReGen4 and Italian Ministry of University and Research for P. Gentile's Ph.D. Grant. Moreover, Dr P. Gentile, is member of the UK EPSRC Centre for Innovative Manufacturing of Medical Devices - MeDe Innovation (EPSRC grant EP/K029592/1).

Figure captions

Figure 1. Chemical Structure of indomethacin (IDMC).

Figure 2. Micrograph of the coated composite scaffold surface after infiltration with a 5% wt/v gelatin solution, incorporating 5 wt. % drug loaded nanoparticles. (Inset) Higher magnification, showing the presence of the IDCM-loaded nanoparticles into the gelatin coating.

Figure 3. FTIR-ATR spectra of uncoated scaffold (A) and gelatin coating scaffold with IDCM-loaded NPs (B). FTIR-ATR resolution: 4 cm^{-1}.

Figure 4. The compressive stress–strain curve of composite scaffold before and after polymeric coating with NPs incorporation. The cross-head speed was set at 0.01 $mm \cdot s^{-1}$. Mean ± SD (n = 3).

Figure 5. Release profile of IDMC from NPs incorporated into the biomimetic coating after immersion in PBS for different times. Mean ± SD (n = 3).

Figure 6. MG-63 osteoblast-like cells attachment and proliferation levels assessed using an MTT method on the fabricated porous composite scaffolds before and after collagen gelatin coating without/with incorporation of indomethacin-loaded PU nanoparticles after 1, 4 and 7 days of culture. Data are represented as the mean ± SD for n= 3, and statistical comparison by Kruskal-Wallis One Way Analysis of Variance on Ranks (ANOVA) showed significant difference at $p < 0.05$ (*).

Figure 7. ALP activity of MG-63 osteoblast-like cells on fabricated porous composite scaffolds before and after collagen gelatin coating without/with incorporation of indomethacin-loaded PU nanoparticles after 14 days of culture. Data are represented as the mean ± SD for n= 3, and statistical comparison by Kruskal-Wallis One Way Analysis of Variance on Ranks (ANOVA) showed significant difference at $p < 0.05$ (*).

References

Bellucci, D., Cannillo, V., Ciardelli, G., Gentile, P., Sola, A., 2010. Potassium based bioactive glass for bone tissue engineering. Ceram Int 36, 2449-2453.
Bellucci, D., Cannillo, V., Sola, A., 2011a. Calcium and potassium addition to facilitate the sintering of bioactive glasses. Mater Lett 65, 1825-1827.
Bellucci, D., Cannillo, V., Sola, A., 2011b. A New Highly Bioactive Composite for Scaffold Applications: A Feasibility Study. Materials 4, 339-354.
Bellucci, D., Chiellini, F., Ciardelli, G., Gazzarri, M., Gentile, P., Sola, A., Cannillo, V., 2012a. Processing and characterization of innovative scaffolds for bone tissue engineering. J Mater Sci-Mater M 23, 1397-1409.
Bellucci, D., Sola, A., Cannillo, V., 2012b. Low Temperature Sintering of Innovative Bioactive Glasses. J Am Ceram Soc 95, 1313-1319.
Bellucci, D., Sola, A., Cannillo, V., 2013a. Bioactive glass-based composites for the production of dense sintered bodies and porous scaffolds. Mat Sci Eng C-Mater 33, 2138-2151.
Bellucci, D., Sola, A., Gazzarri, M., Chiellini, F., Cannillo, V., 2013b. A new hydroxyapatite-based biocomposite for bone replacement. Mat Sci Eng C-Mater 33, 1091-1101.
Bellucci, D., Sola, A., Gentile, P., Ciardelli, G., Cannillo, V., 2012c. Biomimetic coating on bioactive glass-derived scaffolds mimicking bone tissue. J Biomed Mater Res A 100A, 3259-3266.
Boccaccini, A.R., Chen, Q., Lefebvre, L., Gremillard, L., Chevalier, J., 2007. Sintering, crystallisation and biodegradation behaviour of Bioglass (R)-derived glass-ceramics. Faraday Discuss 136, 27-44.
Cabezas, L.I., Fernandez, V., Mazarro, R., Gracia, I., de Lucas, A., Rodriguez, J.F., 2012. Production of biodegradable porous scaffolds impregnated with indomethacin in supercritical CO2. J Supercrit Fluid 63, 155-160.
Chen, H.M., Ouyang, W., Martoni, C., Afkhami, F., Lawuyi, B., Lim, T., Prakash, S., 2010. Investigation of Genipin Cross-Linked Microcapsule for Oral Delivery of Live Bacterial Cells and Other Biotherapeutics: Preparation and In Vitro Analysis in Simulated Human Gastrointestinal Model. Int J Polym Sci.
Chen, Q.Z.Z., Thompson, I.D., Boccaccini, A.R., 2006a. 45S5 Bioglass (R)-derived glass-ceramic scaffolds for bone tissue engineering. Biomaterials 27, 2414-2425.
Chen, Y., Mak, A.F.T., Wang, M., Li, J.S., Wong, M.S., 2006b. PLLA scaffolds with biomimetic apatite coating and biomimetic apatite/collagen composite coating to enhance osteoblast-like cells attachment and activity. Surf Coat Tech 201, 575-580.
Chen, Y.S., Chang, J.Y., Cheng, C.Y., Tsai, F.J., Yao, C.H., Liu, B.S., 2005. An in vivo evaluation of a biodegradable genipin-cross-linked gelatin peripheral nerve guide conduit material. Biomaterials 26, 3911-3918.
Ciardelli, G., Gentile, P., Chiono, V., Mattioli-Belmonte, M., Vozzi, G., Barbani, N., Giusti, P., 2010. Enzymatically crosslinked porous composite matrices for bone tissue regeneration. J Biomed Mater Res A 92A, 137-151.
Cihlar, J., Buchal, A., Trunec, M., 1999. Kinetics of thermal decomposition of hydroxyapatite bioceramics. J Mater Sci 34, 6121-6131.
Day, R.M., 2005. Bioactive glass stimulates the secretion of angiogenic growth factors and angiogenesis in vitro. Tissue Eng 11, 768-777.
Ducheyne, P., Radin, S., King, L., 1993. The effect of calcium phosphate ceramic composition and structure on in vitro behavior. I. Dissolution. J Biomed Mater Res 27, 25-34.
Ferreira, A.M., Mattu, C., Ranzato, E., Ciardelli, G., 2014. Bioinspired porous membranes containing polymer nanoparticles for wound healing. J Biomed Mater Res A.
Gentile, P., Chiono, V., Boccafoschi, F., Baino, F., Vitale-Brovarone, C., Verne, E., Barbani, N., Ciardelli, G., 2010. Composite Films of Gelatin and Hydroxyapatite/Bioactive Glass for Tissue-Engineering Applications. J Biomat Sci-Polym E 21, 1207-1226.
Gibson, L.J., Ashby, M.F., Karam, G.N., Wegst, U., Shercliff, H.R., 1995. The Mechanical-Properties of Natural Materials .2. Microstructures for Mechanical Efficiency. P R Soc-Math Phys Sc 450, 141-162.
Goller, G., Demirkiran, H., Oktar, F.N., Demirkesen, E., 2003. Processing and characterization of bioglass reinforced hydroxyapatite composites. Ceram Int 29, 721-724.
Golub, E.E., Harrison, G., Taylor, A.G., Camper, S., Shapiro, I.M., 1992. The Role of Alkaline-Phosphatase in Cartilage Mineralization. Bone Miner 17, 273-278.
Huang, K.S., Lu, K., Yeh, C.S., Chung, S.R., Lin, C.H., Yang, C.H., Dong, Y.S., 2009. Microfluidic controlling monodisperse microdroplet for 5-fluorouracil loaded genipin-gelatin microcapsules. J Control Release 137, 15-19.
Huang, Y., Onyeri, S., Siewe, M., Moshfeghian, A., Madihally, S.V., 2005. In vitro characterization of chitosan-gelatin scaffolds for tissue engineering. Biomaterials 26, 7616-7627.
Idowu, B., Cama, G., Deb, S., Di Silvio, L., 2014. In vitro osteoinductive potential of porous monetite for bone tissue engineering. J Tissue Eng 5, 2041731414536572.
Kazarian, S.G., Chan, K.L.A., Maquet, V., Boccaccini, A.R., 2004. Characterisation of bioactive and resorbable polylactide/Bioglass((R)) composites by FTIR spectroscopic imaging. Biomaterials 25, 3931-3938.
Kim, I.S., Jeong, Y.I., Cho, C.S., Kim, S.H., 2000. Core-shell type polymeric nanoparticles composed of poly(L-lactic acid) and poly(N-isopropylacrylamide). Int J Pharm 211, 1-8.

Krajewski, A., Mazzocchi, M., Buldini, P.L., Ravaglioli, A., Tinti, A., Taddei, P., Fagnano, C., 2005. Synthesis of carbonated hydroxyapatites: efficiency of the substitution and critical evaluation of analytical methods. J Mol Struct 744, 221-228.
Kuijpers, A.J., Engbers, G.H.M., Krijgsveld, J., Zaat, S.A.J., Dankert, J., Feijen, J., 2000. Cross-linking and characterisation of gelatin matrices for biomedical applications. J Biomat Sci-Polym E 11, 225-243.
Langer, R., Vacanti, J.P., 1993. Tissue Engineering. Science 260, 920-926.
LeGeros, R.Z., 2002. Properties of osteoconductive biomaterials: Calcium phosphates. Clin Orthop Relat R, 81-98.
Manjoo, A., Sanders, D., Lawendy, A., Gladwell, M., Gray, D., Parry, N., Badhwar, A., 2010. Indomethacin Reduces Cell Damage: Shedding New Light on Compartment Syndrome. Journal of Orthopaedic Trauma 24, 526-529.
Mattu, C., Boffito, M., Sartori, S., Ranzato, E., Bernardi, E., Sassi, M.P., Di Rienzo, A.M., Ciardelli, G., 2012. Therapeutic nanoparticles from novel multiblock engineered polyesterurethanes. J Nanopart Res 14.
Mattu, C., Pabari, R.M., Boffito, M., Sartori, S., Ciardelli, G., Ramtoola, Z., 2013. Comparative evaluation of novel biodegradable nanoparticles for the drug targeting to breast cancer cells. Eur J Pharm Biopharm 85, 463-472.
Oonishi, H., Hench, L.L., Wilson, J., Sugihara, F., Tsuji, E., Matsuura, M., Kin, S., Yamamoto, T., Mizokawa, S., 2000. Quantitative comparison of bone growth behavior in granules of Bioglass, A-W glass-ceramic, and hydroxyapatite. J Biomed Mater Res 51, 37-46.
Orlovskii, V.P., Komlev, V.S., Barinov, S.M., 2002. Hydroxyapatite and hydroxyapatite-based ceramics. Inorg Mater+ 38, 973-984.
Ravarian, R., Moztarzadeh, F., Hashjin, M.S., Rabiee, S.M., Khoshakhlagh, P., Tahriri, M., 2010. Synthesis, characterization and bioactivity investigation of bioglass/hydroxyapatite composite. Ceram Int 36, 291-297.
Rezwan, K., Chen, Q.Z., Blaker, J.J., Boccaccini, A.R., 2006. Biodegradable and bioactive porous polymer/inorganic composite scaffolds for bone tissue engineering. Biomaterials 27, 3413-3431.
Suchanek, W., Yashima, M., Kakihana, M., Yoshimura, M., 1997. Hydroxyapatite ceramics with selected sintering additives. Biomaterials 18, 923-933.
Temussi, F., Cermola, F., DellaGreca, M., Iesce, M.R., Passananti, M., Previtera, L., Zarrelli, A., 2011. Determination of photostability and photodegradation products of indomethacin in aqueous media. J Pharmaceut Biomed 56, 678-683.
Thakur, G., Mitra, A., Basak, A., Sheet, D., 2012. Characterization and scanning electron microscopic investigation of crosslinked freeze dried gelatin matrices for study of drug diffusivity and release kinetics. Micron 43, 311-320.
Tonda-Turo, C., Gentile, P., Saracino, S., Chiono, V., Nandagiri, V.K., Muzio, G., Canuto, R.A., Ciardelli, G., 2011. Comparative analysis of gelatin scaffolds crosslinked by genipin and silane coupling agent. Int J Biol Macromol 49, 700-706.
Vitale-Brovarone, C., Verne, E., Robiglio, L., Martinasso, G., Canuto, R.A., Muzio, G., 2008. Biocompatible glass-ceramic materials for bone substitution. J Mater Sci-Mater M 19, 471-478.
Xynos, I.D., Hukkanen, M.V.J., Batten, J.J., Buttery, L.D., Hench, L.L., Polak, J.M., 2000. Bioglass (R) 45S5 stimulates osteoblast turnover and enhances bone formation in vitro: Implications and applications for bone tissue engineering. Calcified Tissue Int 67, 321-329.

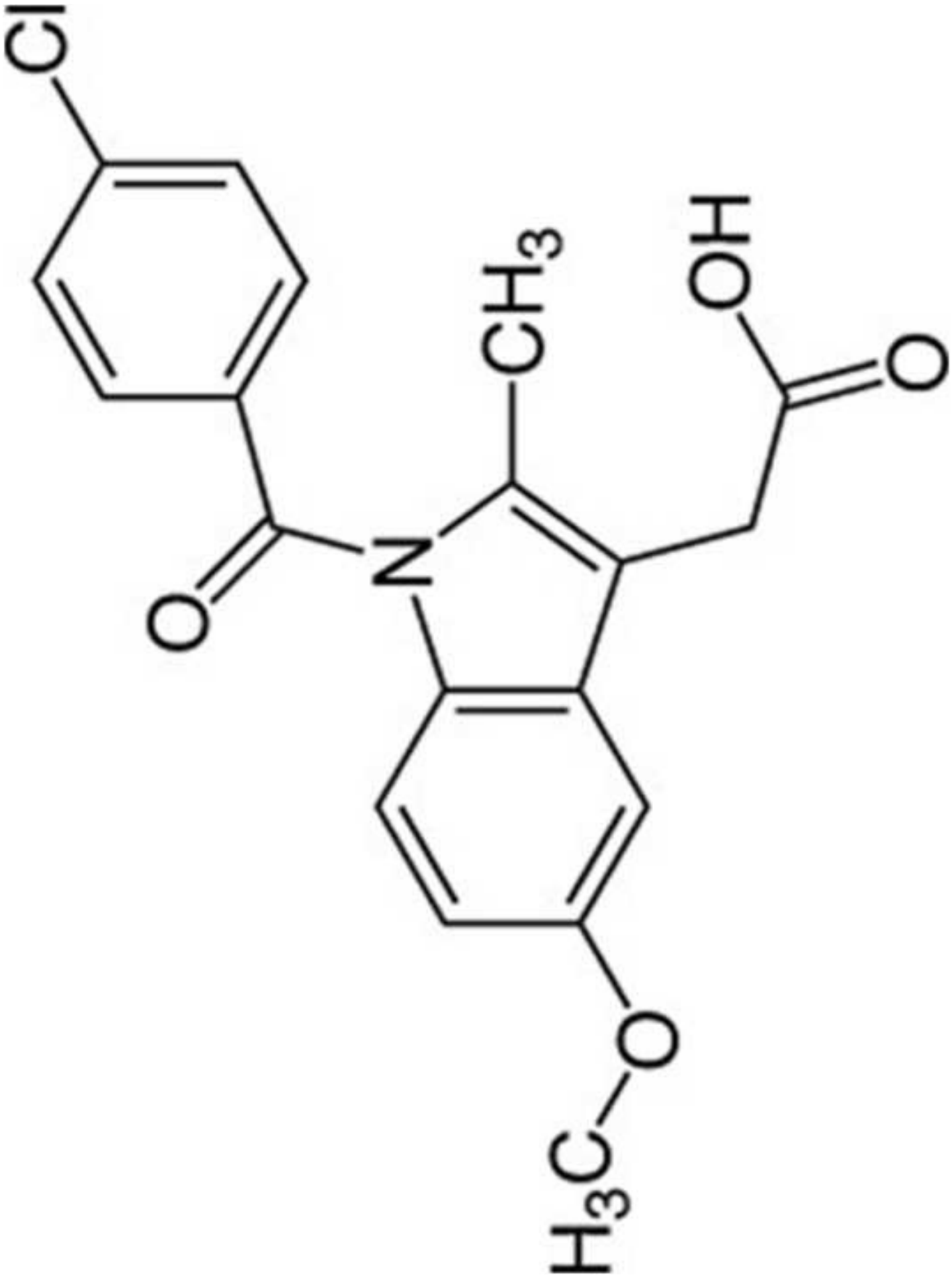

Figure 1

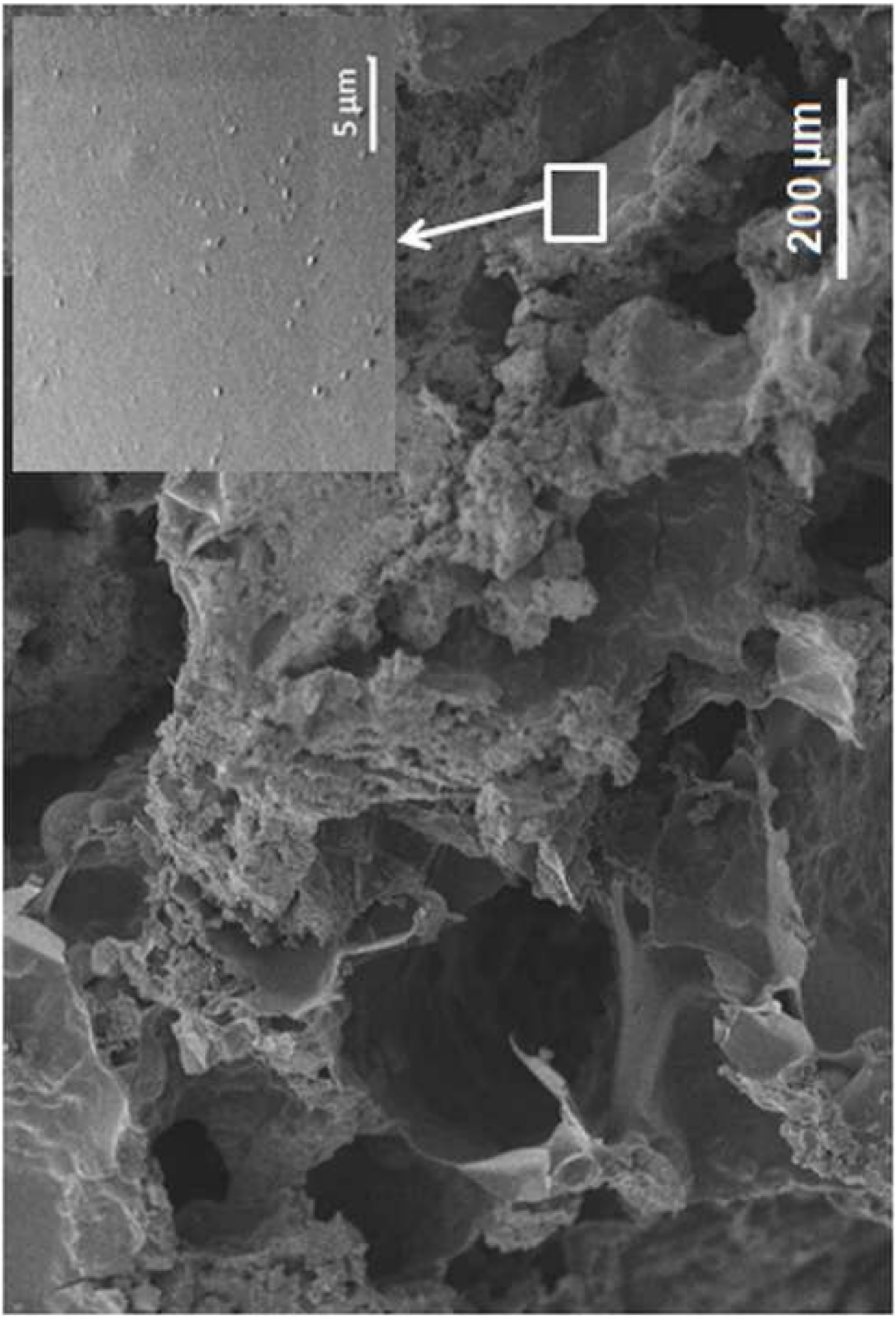

Figure 2

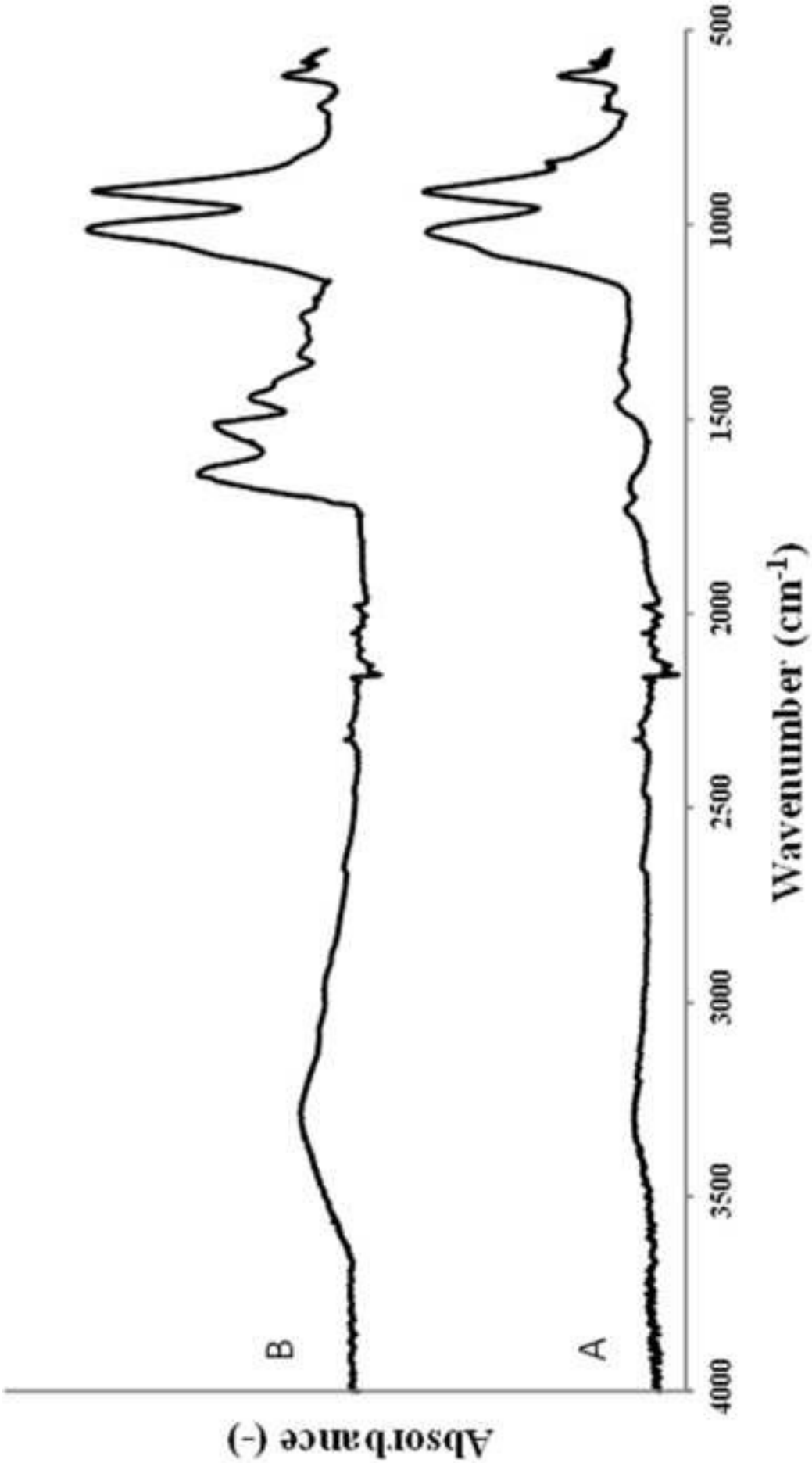

Figure 3

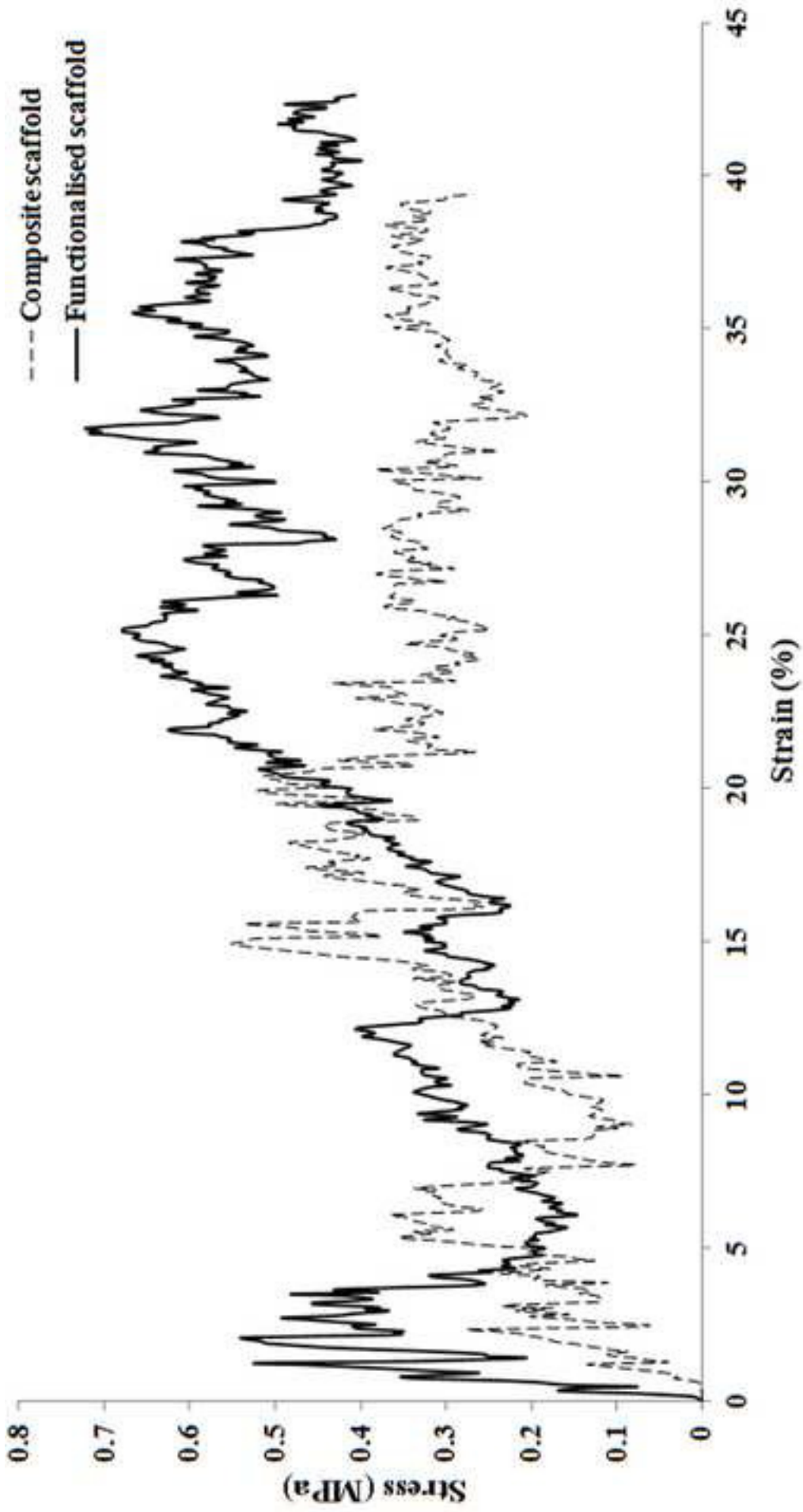

Figure 4

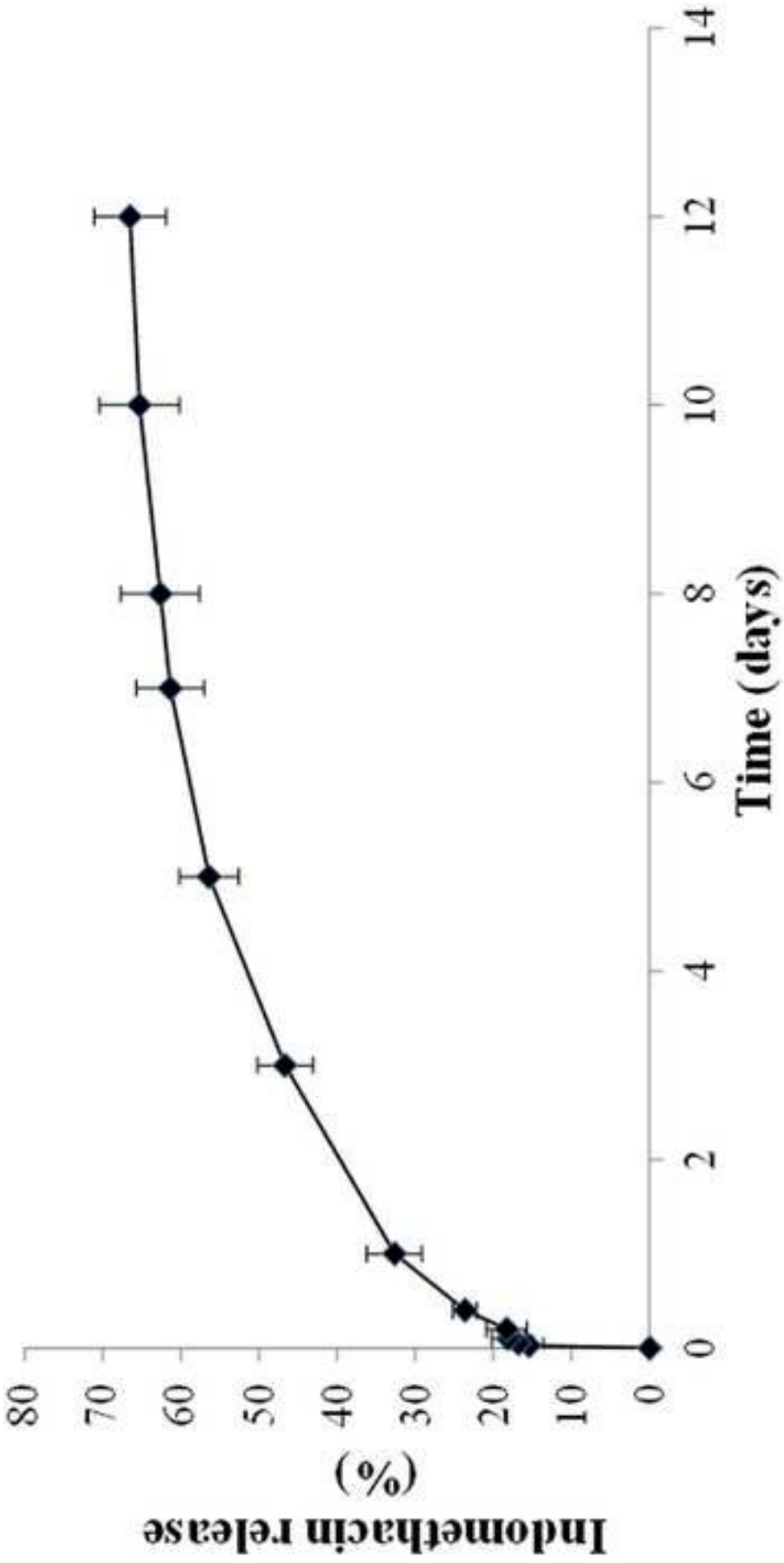
Indomethacin release
(%)
80
70
60
50
40
30
20
10
0
0
2
4
6
8
10
12
14
Time (days)

Figure 5

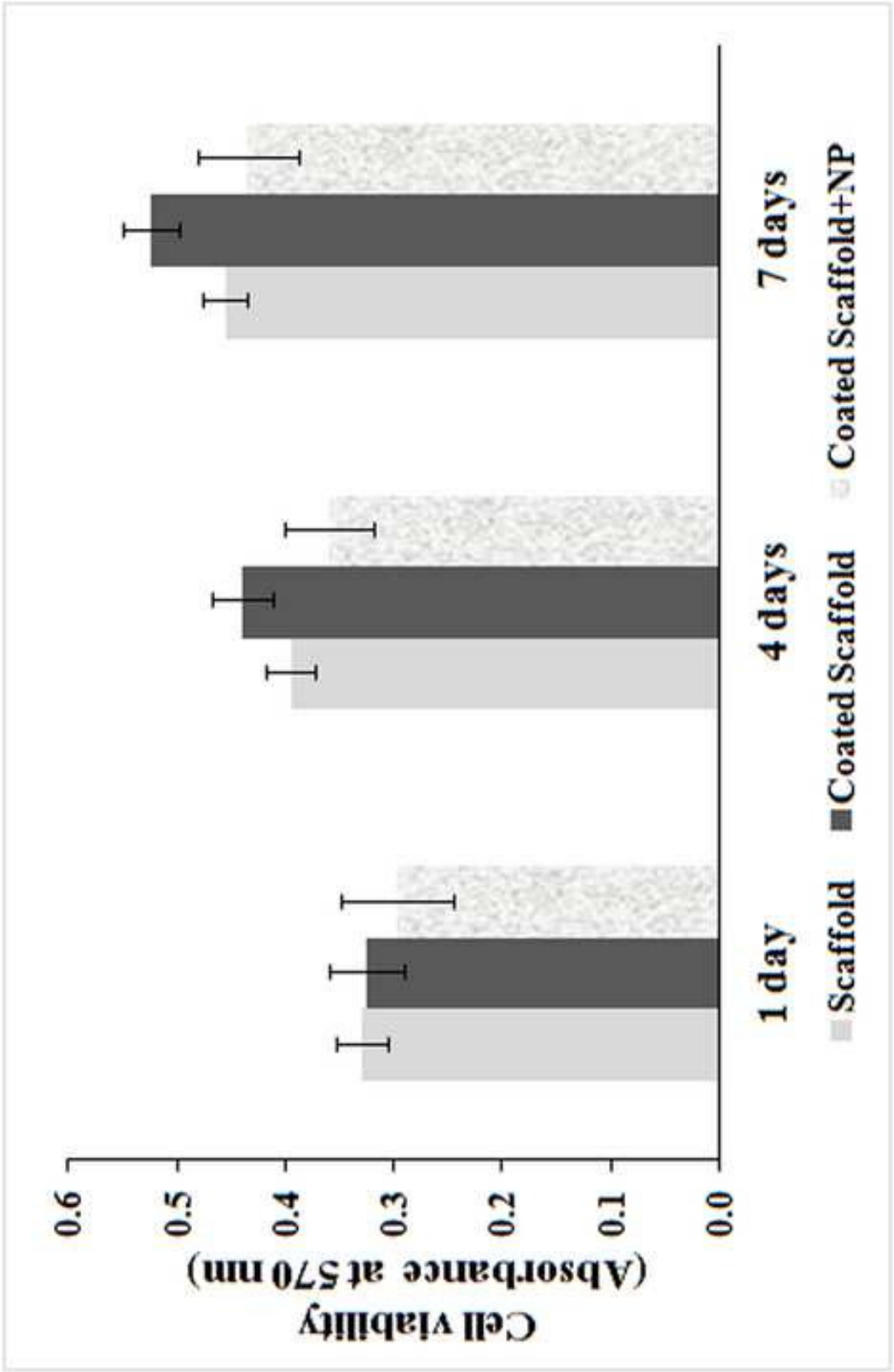
Cell viability
(Absorbance at 570 nm)
0.0
0.1
0.2
0.3
0.4
0.5
0.6
1 day
4 days
7 days
Scaffold
Coated Scaffold
Coated Scaffold+NP

Figure 6

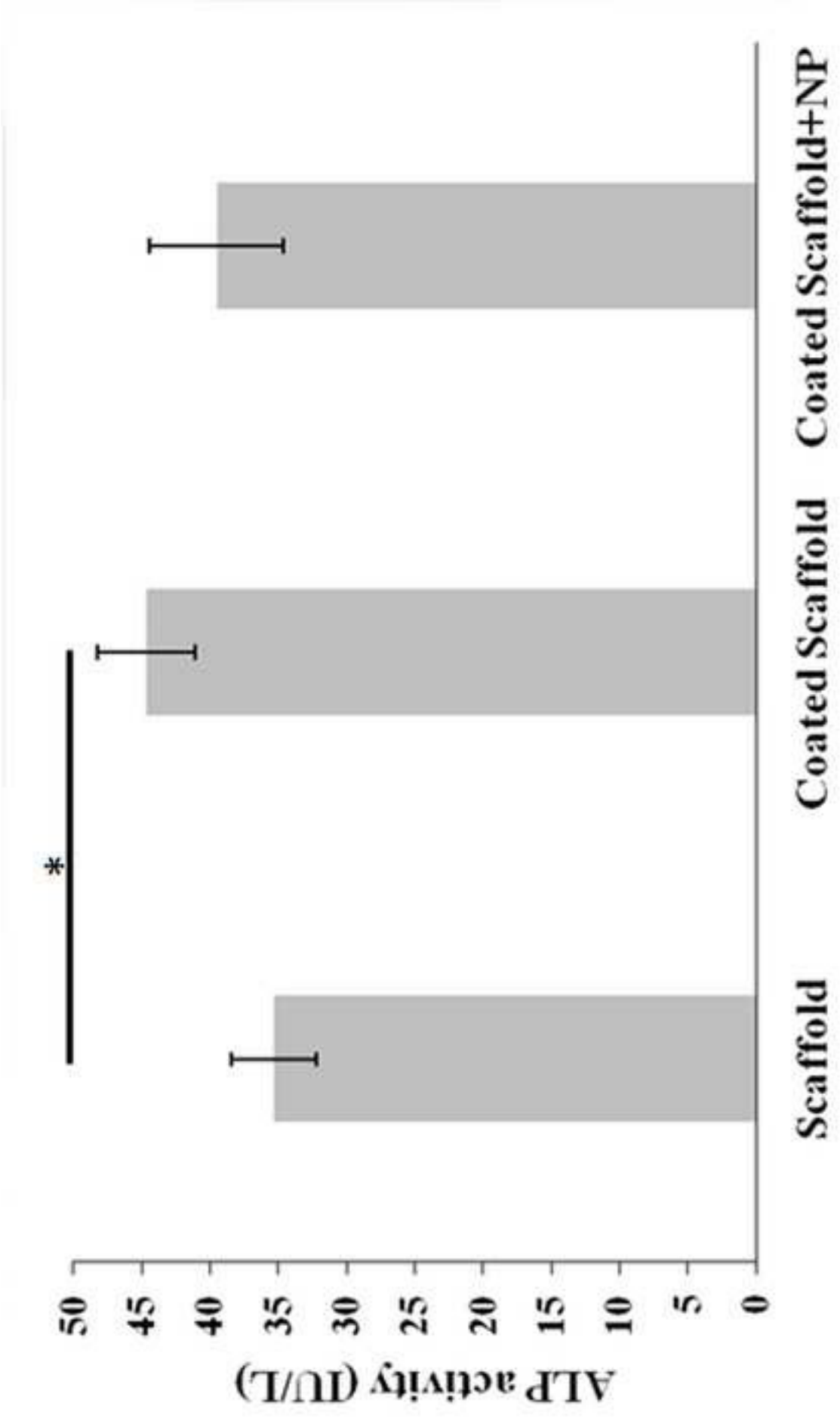
ALP activity (IU/L)
0
5
10
15
20
25
30
35
40
45
50
*
Scaffold
Coated Scaffold
Coated Scaffold+NP

Figure 7